Published in final edited form as:
Int J Radiat Oncol Biol Phys. 2009 February 1; 73(2): 523–529. doi:10.1016/j.ijrobp.2008.09.036.

Radiation-induced salivary gland dysfunction results from p53-dependent apoptosis

Jennifer L. Avila, MS[1], **Oliver Grundmann, PhD**[2], **Randy Burd, PhD**[2], and **Kirsten H. Limesand, PhD**[1,2,*]

1 *Physiological Sciences, University of Arizona, Tucson, AZ*

2 *Department of Nutritional Sciences, University of Arizona, Tucson, AZ*

Abstract

Purpose—Radiation therapy for head and neck cancer causes adverse secondary side effects in the salivary glands and results in diminished quality of life for the patient. A previous *in vivo* study in parotid salivary glands demonstrated that targeted head and neck irradiation resulted in marked increases in phosphorylated p53 (serine[18]) and apoptosis, which was suppressed in transgenic mice expressing a constitutively active mutant of Akt1 (myr-Akt1).

Methods and Materials—Transgenic and knockout mouse models were exposed to irradiation and p53-mediated transcription, apoptosis, and salivary gland dysfunction were analyzed.

Results—We report that the pro-apoptotic p53 target genes PUMA and Bax are induced in parotid salivary glands of mice at early time points following therapeutic radiation. This dose-dependent induction requires expression of p53 as no radiation-induced expression of PUMA and Bax is observed in p53−/− mice. Radiation also induces apoptosis in the parotid gland in a dose dependent manner, which is p53-dependent. Furthermore, expression of p53 is required for the acute and chronic loss of salivary function following irradiation. In contrast, p53−/− mice do not induce apoptosis and preserve salivary function after radiation exposure.

Conclusion—These results indicate that apoptosis in the salivary glands following therapeutic head and neck irradiation is mediated by p53 and corresponds to salivary gland dysfunction *in vivo*.

INTRODUCTION

Therapeutic radiation is used for the treatment of head and neck cancer and commonly results in unwanted secondary side effects in normal salivary glands. These side effects include xerostomia, oral mucositis, and increased risk of periodontal disease resulting in diminished quality of life for these patients (1). Clinically, parotid salivary glands appear to be more radiosensitive than submandibular salivary glands (2–4), which has also been reported in animal models (5;6). Submandibular glands contribute approximately two-thirds of unstimulated saliva volume, whereas parotid glands contribute the majority of stimulated saliva volume (7;8).

*Corresponding Author: Kirsten H. Limesand, 1177 E 4th St, Shantz 421, Tucson, AZ 85721, Phone (520) 626-4517, Fax: (520) 621-9446, Email: limesank@u.arizona.edu.

Conflict of Interest Notification. Conflicts of interest do not exist for any of the authors.

Irradiation of the salivary glands causes a significant loss of acinar cells; however the mechanisms of this cellular attrition have been widely debated. Earlier work in a rat model quantified radiation-induced apoptosis by counting condensed nuclei and reported 2–3% apoptotic cells six hours after treatment with a broad range of doses (2.5–25 Gy) (9). The extent of apoptosis was not dose dependent and the authors concluded that the magnitude of apoptosis could not explain the significant loss of function (9). In contrast to rats, radiation-induced apoptosis is dose dependent in parotid glands of mice with significantly higher levels detected using immunohistochemistry against activated caspase-3 (5;10). The relevance of radiation-induced apoptosis to the overall physiological function of the salivary gland has not yet been elucidated.

Akt (protein kinase B) is a serine/threonine protein kinase that activates important survival signals in numerous tissues through a number of substrates (11). In primary salivary acinar cells, expression of the Akt substrate *Murine Double Minute Clone 2* (MDM2) is required for suppression of DNA damage-induced apoptosis (10). Phosphorylation of MDM2 by Akt enhances its translocation to the nucleus, where it binds to p53 and targets p53 for degradation by the proteasome (12). DNA damage leads to p53 protein accumulation and transcriptional activation resulting in the induction of cell cycle arrest or apoptotic target genes (13). Among these p53 target genes are the pro-apoptotic Bcl-2 family members PUMA (p53 up-regulated modulator of apoptosis) and Bax (Bcl-2-associated X protein). PUMA interacts with Bax eventually leading to apoptosis (14) suggesting cooperative action of multiple p53 pro-apoptotic target genes (13). PERP (p53 apoptosis effector related to PMP-22), like Bax and PUMA, is a p53 target gene induced by DNA damage that may have pro-apoptotic effects (15). Elucidating the pathways activated following therapeutic radiation in the salivary glands will help determine the mechanism of dysfunction and potentially aid in the development of specific treatment options.

In this study, we observe a dose-dependent shift in PUMA and Bax mRNA expression in parotid salivary glands following irradiation in transgenic mice expressing a constitutively activated mutant of Akt1 (myr-Akt1) compared to FVB wildtype. In order to elucidate the specific role of p53 in salivary gland dysfunction, we used a genetically engineered mouse model containing a targeted deletion of p53 (p53−/−) (16). p53+/+ and p53+/− mice show a dose-dependent increase in transcription of pro-apoptotic genes (PUMA and Bax), which correlates with an increase in activated caspase-3. In contrast, p53−/− mice exhibit no change in expression of these pro-apoptotic genes or caspase-3 activation following irradiation. Apoptosis in the p53+/+ and p53+/− mice correlates with a significant decrease in stimulated salivary flow rates, indicative of salivary dysfunction, which is not observed in p53−/− mice. Our data support the hypothesis that p53 mediates an apoptotic pathology in normal salivary glands *in vivo*.

MATERIALS AND METHODS

Mice

Myr-Akt1 transgenic mice under the control of the mouse mammary tumor virus promoter and maintained on an FVB background, were generated at the University of Colorado Health Sciences Center (17) and the salivary gland phenotype was described previously (10). p53 knockout mice were provided by Dr. Carla van den Berg (University of Texas at Austin), maintained on a Balb/c background, and genotyped using PCR (16). Primers used for genotyping were obtained from Integrated DNA Technologies (Coralville, IA).

Radiation Treatment

Four-week-old female FVB, myr-Akt1, or p53 mice from each genotype were anesthetized with avertin (0.4 to 0.6 mg/kg, intraperitoneally [i.p.]), and the head and neck region was exposed to radiation [Cobalt-60 Teletherapy unit from Atomic Energy of Canada Ltd Theratron-80] as previously described (10). Animals were maintained and treated in accordance with protocols approved by the University of Arizona IACUC.

RNA isolation and real-time RT-PCR

Parotid glands were removed from irradiated FVB, myr-Akt1, and p53 female mice (1, 2, or 5 Gy treatments) and RNA was isolated as previously described (10). 1 μg of RNA was reverse transcribed with a Super Script III kit according to manufacturer's instructions (Invitrogen, Carlsbad, CA) and real-time RT-PCR was conducted in triplicate for each cDNA sample (3–5 mice per genotype per dose) with an iQ5 Real-Time PCR Detection System (BioRad, Hercules, CA). Forty cycles of PCR were performed (95°C for 15 seconds, 54°C for 30 seconds, 72°C for 30 seconds); fluorescence detection occurred during the 72°C step at each cycle. The data were analyzed using the $2^{-\Delta\Delta Ct}$ method (18). Results were normalized to S15, which remains unchanged in response to treatment. Normalized values were plotted as relative fold over untreated wildtype. The following primers were purchased from Integrated DNA Technologies: S15 (10), PUMA (forward, 5′-CGT GTG ACC ACT GGC ATT CAT T-3′; reverse, 5′-ACA CAC ACA CAC ACA CAC ACA C-3′), PERP (19). QuantiTect Bax primers were purchased from Qiagen.

Histology

Tissues were fixed in 10% neutral buffered formalin for 24 hours, transferred to 70% ethanol, and embedded in paraffin. Tissue sections were cut to 4 μm and processed for standard staining with hematoxylin and eosin by the Histology Service Laboratory in the Department of Cell Biology and Anatomy at the University of Arizona.

Induction and quantification of apoptosis

Salivary glands were removed 24, 48, 72, and 96 hours post-irradiation and processed for histology as described above. Unstained tissue sections were processed for anti-activated caspase-3 immunohistochemistry as previously described (10). Tissue sections were observed by standard light microscopy, and photomicrographs were taken with a Leica DM5500 with a 4 megapixel Pursuit camera. Individual means for quantification of caspase-3 positive cells were determined by averaging the number of positive cells/total number of cells from a minimum of three fields of view/animal (2–3 mice per genotype per treatment; total cells counted ranged from 2,400 to 3,400 per field of view).

Saliva Collection

Mice were injected i.p. with 0.25 mg carbachol per kg body weight as previously described (10) on day 3 and 30 after radiation treatments. Saliva was collected from 8–10 mice/genotype/treatment on ice immediately following carbachol injection for 5 min into pre-weighed tubes and stored at −80°C.

Statistics

Comparison of real-time RT-PCR and caspase-3 data was accomplished by a one-way ANOVA followed by a Bonferroni test with adjustment for the number of pairwise comparisons. Saliva flow rates were analyzed using a one-way ANOVA followed by Tukey's multiple comparison test. Statistical analysis and graphical generation of data were done using GraphPad Prism software (San Diego, CA).

RESULTS

Pro-apoptotic p53 target genes are induced in parotid salivary glands following therapeutic radiation

A previous study in parotid salivary glands demonstrated that targeted head and neck irradiation resulted in marked increases in phosphorylated p53 (serine^{18}) and apoptosis eight hours after treatment, which were inhibited in transgenic mice expressing myr-Akt1 (10). These data indicated that a rapid apoptotic response to DNA damage in the salivary glands may involve activation of p53 target genes. To investigate this we looked at the expression of two important pro-apoptotic transcriptional targets of p53 (PUMA and Bax) in parotid salivary glands following head and neck irradiation using the myr-Akt1 transgenic mouse line.

After irradiation, in both wildtype (FVB) and myr-Akt1 mice, PUMA expression is significantly up-regulated at 4 hours post treatment at doses of 2 and 5 Gy compared to genotype specific untreated controls (Fig. 1A). In myr-Akt1 transgenic mice eight hours after treatment, there appears to be a shift in the dose response curves for PUMA mRNA expression as evidenced by the significant reduction at 5 Gy compared to FVB wildtype (Fig. 1B). Induction of Bax follows a similar profile as PUMA at both time points (Fig. 1C,D). These data indicate a rapid induction of PUMA and Bax following irradiation that was modulated by myr-Akt1 eight hours after treatment. Reductions in radiation-induced p53 phosphorylation by Akt (10) correlates with the reductions in PUMA and Bax expression, which suggests a potential role for Akt in modulating p53 transcriptional activity *in vivo*.

Radiation-induced expression of PUMA and Bax depends on p53

To investigate the role of p53 in the induction of PUMA and Bax following radiation-induced DNA damage, we used a genetically engineered mouse model with a targeted deletion of p53 (16). p53+/+, p53+/−, and p53−/− mice were irradiated with 1, 2, or 5 Gy targeted to the head and neck region. Parotid salivary glands were collected 4 hours after treatment and expression of p53 pro-apoptotic genes was quantified by real-time RT-PCR. PUMA mRNA expression in irradiated p53+/+ and p53+/− mice is dose dependent with significant increases at 2 and 5 Gy compared to the respective untreated genotype (Fig. 2A). In both p53+/+ and +/− mice, maximal induction of PUMA is observed following 5 Gy, similar to the trend in FVB mice (Fig. 1A). PUMA expression in p53−/− mice appears to increase at 5 Gy; however, this is not significant due to slightly higher basal levels in untreated p53-/− mice. Bax mRNA expression follows a dose dependent trend in both p53+/+ and p53+/− mice with significant increases at all doses for p53+/+ and at 2 and 5 Gy for p53+/− (Fig. 2B). In contrast, there are no significant changes in expression of Bax following treatment in p53−/− mice.

PERP is not induced in the parotid salivary gland following irradiation

Induction of PERP following irradiation is p53-dependent and has been shown to contribute to apoptosis in neurons and thymocytes (15). In the salivary glands of mice treated with therapeutic radiation, there is no induction of PERP expression after four hours at any of the doses examined in the p53 genotypes (Fig. 3). This response is not mouse strain-dependent as there is no significant increase in PERP expression following radiation in p53+/+ mice maintained on a Balb/c genetic background or FVB wildtype mice (data not shown). These data do not provide evidence for involvement of PERP in the apoptotic response of parotid salivary glands to therapeutic radiation.

Radiation-induced apoptosis in the parotid gland is p53-dependent

In order to determine the necessity of p53 for radiation-induced apoptosis in the salivary glands, p53+/+, p53+/−, and p53−/− mice were exposed to 1, 2, 5, or 10 Gy radiation targeted to the

head and neck region. As depicted in Figure 4A, we observe a dose-dependent increase in the number of apoptotic cells 24h after treatment in p53+/+ and +/− mice, as determined by activated caspase-3 positive cells, which is significant following 5 and 10 Gy. Interestingly, there is a significantly higher number of apoptotic cells in p53+/+ compared to p53+/− parotid salivary glands treated with 10 Gy. In contrast, p53−/− mice have no radiation-induced apoptosis at any dose of radiation we examined.

In order to determine the kinetics of salivary gland apoptosis, we evaluated caspase-3 activation at various time points after 5 Gy irradiation in all p53 genotypes (Fig. 4B). The peak number of apoptotic cells is observed between 24 and 48 hours in both p53+/+ and p53+/− mice. The number of apoptotic cells drops dramatically at 72 and 96 hours presumably due to clearance of these cells. No significant induction of apoptosis is observed in p53−/− mice at any of the time points. A majority (>95%) of the apoptotic cells counted for figures 4A and B are acinar cells. These data indicate that p53-independent apoptosis that has been observed in other tissues (20) is not prevalent in parotid salivary glands within 96 hours of treatment.

p53-dependent apoptosis affects salivary function

Acute and chronic reductions in salivary flow rates following radiation have been reported in rats (6;21), rhesus monkeys (22), and humans (23); however, the pathways to preserve function have remained elusive. In order to determine if salivary function is related to p53-dependent apoptosis, mice from all p53 genotypes were irradiated with 2 or 5 Gy and stimulated flow rates were determined on days 3 and 30. Radiation doses for functional studies were chosen based on clinical exposure of the salivary glands is typically kept below 2 Gy/day (24;25) and to correlate function with the induction of apoptosis (Fig. 4A).

Stimulated salivary flow rates are significantly reduced on day 3 in 2 Gy irradiated p53+/+ and p53+/− mice compared to genotype specific untreated mice (Fig. 5A). Remarkably, we observe similar decreases in stimulated salivary flow rates in p53+/+ mice after radiation with 5 Gy (Fig. 5B). The diminished salivary flow observed in our mouse model (~30–45%) is similar to previous studies using irradiated rats (~40–60%) (6;9;21). In contrast, p53−/− mice have no significant reduction in salivary flow at either dose of radiation examined. Early reductions in salivary flow rates therefore might be related to an apoptotic stress response mediated by p53 (Fig. 4B).

Mice were re-evaluated after 30 days to determine if salivary gland hypofunction persisted in response to radiation. Both p53+/+ and p53+/− mice have significantly decreased flow rates compared to untreated mice following exposure to either radiation dose (Fig. 6A,B). In contrast, p53−/− mice treated with therapeutic doses of radiation show little change in salivary flow rates. The significant reduction in saliva flow rate in p53+/+ and p53+/− mice at 2 and 5 Gy implies at least a 2 Gy threshold response to radiation in the salivary glands. These data suggest that expression of p53 is essential in the acute and chronic loss of salivary function following exposure to therapeutic radiation.

DISCUSSION

Considerable uncertainty exists about the mechanisms of radiation-induced damage in salivary glands. Studies using a rat model reported significant decreases in salivary gland flow rates without a significant increase in apoptotic cells (9). However, our results indicate that modulation of the apoptotic response following therapeutic radiation preserves salivary gland function at both acute and chronic time points (Fig. 5 and 6). This suggests that radiation-induced apoptosis of salivary acinar cells correlates with salivary dysfunction. These data also indicate that apoptosis may have a more significant role in the impairment of function of the salivary glands following radiation exposure than previously reported. Interestingly, radiation-

induced salivary gland dysfunction was not different between the two doses evaluated (Fig. 6; 2 and 5 Gy). This may indicate that there is a threshold of radiation sensitivity in mice at doses that parallel the salivary gland exposure in patients treated for head and neck cancer (i.e., 1.8–2.0 Gy/day) (24;25).

In our study we report that a significant induction of apoptosis (Fig. 4) occurs in parotid salivary glands exposed to radiation in mice expressing at least one allele of p53. The lack of apoptosis in parotid salivary glands and preservation of salivary flow in p53−/− mice within our study supports a role for p53 in an apoptotic pathology of the salivary glands. Our results concur with previous studies in other tissues (26;27), showing an inhibition of p53 may be beneficial in protecting radiosensitive tissues during therapeutic radiation treatment. These studies, along with our own, support the possibility that temporary inhibition of p53, through the use of molecules such as pifithrin-α, prior to irradiation may benefit patients through protection from adverse secondary side effects.

Regulation of p53's functions in inducing apoptosis may lie in two different mechanisms: induction of apoptotic genes (13;28) or translocation to the mitochondria (29). While our study did not address p53 localization, this mechanism has been shown to occur *in vivo* (30) and occurs in the absence of transcription (31). A previous study in primary salivary acinar cells identified a critical role for the Akt/MDM2/p53 pathway in suppression of DNA damage-induced apoptosis (10). In mice expressing the myr-Akt1 transgene, we observe a dose-dependent shift in PUMA and Bax mRNA expression in parotid salivary glands following irradiation compared to FVB wildtype mice (Fig. 1B,D). This modulation of PUMA and Bax mRNA expression in myr-Akt1 parotid salivary glands is observed at the eight hour time point consistent with the reduced levels of phosphorylated p53 previously reported at this time point (10). In the p53+/+ and p53+/−mice, PUMA and Bax are significantly increased in the salivary glands following irradiation in a dose-dependent manner; however, there is no significant change in expression in p53−/− mice (Fig. 2). PUMA expression has also been shown to be regulated by p73, a homologue of p53 (32). This possibility could explain the slight (not significant) increase in PUMA mRNA expression in p53−/− parotid salivary glands at higher doses of radiation. As expected, the induction of pro-apoptotic genes resembles the apoptotic response in the parotid salivary glands following therapeutic radiation.

Alternatively, p53 has been shown to regulate the cellular processes of autophagy and senescence. Autophagy ('self-eating') can lead to enhanced cell survival or cell death depending on the tissue type or environmental stressor (33). In tumor models, autophagy is considered a secondary means of cell death when apoptosis has been blocked (34;35). Both activation and inhibition of p53 have been shown to induce autophagy (36;37); therefore, the implications to radiation-induced salivary gland dysfunction are unclear. Radiation-induced DNA damage can also result in p53-dependent senescence (38), which may contribute to the chronic, but not acute, loss of function in the salivary glands. It is likely that apoptosis, autophagy and senescence are present in irradiated salivary glands and may be not mutually exclusive. Future studies will be required to delineate the kinetics of these cellular processes.

Our data demonstrate that modulation of p53 expression (and thereby activation) directly correlates with preservation of salivary gland function. This is the first genetic evidence that links an intracellular pathway to potential mechanisms of radiation-induced salivary gland damage. A limitation of this study would be the use of a single dose of radiation considering that patients receive fractionated doses. By gaining an understanding of the p53-mediated pathways in salivary gland hypofunction we can continue to make strides to improve the overall quality of life of patients suffering from chronic secondary side effects attributed to therapeutic radiation.

Acknowledgements

p53 mice were a gift from Dr. Carla van den Berg (University of Texas at Austin). This work was supported in part by the NIH K22 DE 16096 and start-up funds from the University of Arizona.

Reference List

1. Nagler RM. Effects of head and neck radiotherapy on major salivary glands--animal studies and human implications. In Vivo 2003;17(4):369–375. [PubMed: 12929593]
2. Li Y, Taylor JM, Ten Haken RK, Eisbruch A. The impact of dose on parotid salivary recovery in head and neck cancer patients treated with radiation therapy. Int J Radiat Oncol Biol Phys 2007;67(3):660–669. [PubMed: 17141973]
3. Eisbruch A, Ten Haken RK, Kim HM, Marsh LH, Ship JA. Dose, volume, and function relationships in parotid salivary glands following conformal and intensity-modulated irradiation of head and neck cancer. Int J Radiat Oncol Biol Phys 1999;45(3):577–587. [PubMed: 10524409]
4. Murdoch-Kinch CA, Kim HM, Vineberg KA, Ship JA, Eisbruch A. Dose-Effect Relationships for the Submandibular Salivary Glands and Implications for Their Sparing by Intensity Modulated Radiotherapy. Int J Radiat Oncol Biol Phys. 2008
5. Humphries MJ, Limesand KH, Schneider JC, Nakayama KI, Anderson SM, Reyland ME. Suppression of apoptosis in the PKCdelta null mouse in vivo. J Biol Chem 2006;281(14):9728–9737. [PubMed: 16452485]
6. Nagler RM, Baum BJ, Miller G, Fox PC. Long-term salivary effects of single-dose head and neck irradiation in the rat. Arch Oral Biol 1998;43(4):297–303. [PubMed: 9839705]
7. Ship JA, Fox PC, Baum BJ. How much saliva is enough? ‘Normal’ function defined. J Am Dent Assoc 1991;122(3):63–69. [PubMed: 2019691]
8. de Almeida PDV, Gregio AM, Machado MA, de Lima AA, Azevedo LR. Saliva composition and functions: a comprehensive review. J Contemp Dent Pract 2008;9(3):72–80. [PubMed: 18335122]
9. Paardekooper GM, Cammelli S, Zeilstra LJ, Coppes RP, Konings AW. Radiation-induced apoptosis in relation to acute impairment of rat salivary gland function. Int J Radiat Biol 1998;73(6):641–648. [PubMed: 9690682]
10. Limesand KH, Schwertfeger KL, Anderson SM. MDM2 is required for suppression of apoptosis by activated Akt1 in salivary acinar cells. Mol Cell Biol 2006;26:8840–8856. [PubMed: 16982679]
11. Manning BD, Cantley LC. AKT/PKB signaling: navigating downstream. Cell 2007;129(7):1261–1274. [PubMed: 17604717]
12. Zhou BP, Liao Y, Xia W, Zou Y, Spohn B, Hung MC. HER-2/neu induces p53 ubiquitination via Akt-mediated MDM2 phosphorylation. Nat Cell Biol 2001;3(11):973–982. [PubMed: 11715018]
13. Riley T, Sontag E, Chen P, Levine A. Transcriptional control of human p53-regulated genes. Nat Rev Mol Cell Biol 2008;9(5):402–412. [PubMed: 18431400]
14. Cartron PF, Gallenne T, Bougras G, Gautier F, Manero F, Vusio P, et al. The first alpha helix of Bax plays a necessary role in its ligand-induced activation by the BH3-only proteins Bid and PUMA. Mol Cell 2004;16(5):807–818. [PubMed: 15574335]
15. Ihrie RA, Reczek E, Horner JS, Khachatrian L, Sage J, Jacks T, et al. Perp is a mediator of p53-dependent apoptosis in diverse cell types. Curr Biol 2003;13(22):1985–1990. [PubMed: 14614825]
16. Kuperwasser C, Hurlbut GD, Kittrell FS, Dickinson ES, Laucirica R, Medina D, et al. Development of spontaneous mammary tumors in BALB/c p53 heterozygous mice. A model for Li-Fraumeni syndrome. Am J Pathol 2000;157(6):2151–2159. [PubMed: 11106587]
17. Schwertfeger KL, Richert MM, Anderson SM. Mammary gland involution is delayed by activated Akt in transgenic mice. Mol Endocrinol 2001;15(6):867–881. [PubMed: 11376107]
18. Livak KJ, Schmittgen TD. Analysis of relative gene expression data using real-time quantitative PCR and the 2(−Delta Delta C(T)) Method. Methods 2001;25(4):402–408. [PubMed: 11846609]
19. Wan YY, DeGregori J. The survival of antigen-stimulated T cells requires NFkappaB-mediated inhibition of p73 expression. Immunity 2003;18(3):331–342. [PubMed: 12648451]
20. Gudkov AV, Komarova EA. The role of p53 in determining sensitivity to radiotherapy. Nat Rev Cancer 2003;3(2):117–129. [PubMed: 12563311]

21. Vissink A, 's-Gravenmade EJ, Ligeon EE, Konings WT. A functional and chemical study of radiation effects on rat parotid and submandibular/sublingual glands. Radiat Res 1990;124(3):259–265. [PubMed: 1702228]
22. Stephens LC, King GK, Peters LJ, Ang KK, Schultheiss TE, Jardine JH. Acute and late radiation injury in rhesus monkey parotid glands. Evidence of interphase cell death. Am J Pathol 1986;124(3): 469–478. [PubMed: 3766705]
23. Eisbruch A, Kim HM, Terrell JE, Marsh LH, Dawson LA, Ship JA. Xerostomia and its predictors following parotid-sparing irradiation of head-and-neck cancer. Int J Radiat Oncol Biol Phys 2001;50 (3):695–704. [PubMed: 11395238]
24. Gregoire V, De Neve W, Eisbruch A, Lee N, Van den WD, Van Gestel D. Intensity-modulated radiation therapy for head and neck carcinoma. Oncologist 2007;12(5):555–564. [PubMed: 17522243]
25. Martin E, Deville C, Bonnetain F, Bosset M, Crehange G, Truc G, et al. Intensity-modulated radiation therapy in head and neck cancer: prescribed dose, clinical challenges and results. Radiother Oncol 2007;85(3):392–398. [PubMed: 18036690]
26. Komarova EA, Chernov MV, Franks R, Wang K, Armin G, Zelnick CR, et al. Transgenic mice with p53-responsive lacZ: p53 activity varies dramatically during normal development and determines radiation and drug sensitivity in vivo. EMBO J 1997;16(6):1391–1400. [PubMed: 9135154]
27. Komarov PG, Komarova EA, Kondratov RV, Christov-Tselkov K, Coon JS, Chernov MV, et al. A chemical inhibitor of p53 that protects mice from the side effects of cancer therapy. Science 1999;285 (5434):1733–1737. [PubMed: 10481009]
28. Oda K, Arakawa H, Tanaka T, Matsuda K, Tanikawa C, Mori T, et al. p53AIP1, a potential mediator of p53-dependent apoptosis, and its regulation by Ser-46-phosphorylated p53. Cell 2000;102(6):849–862. [PubMed: 11030628]
29. Mihara M, Moll UM. Detection of Mitochondrial Localization of p53. Methods Mol Biol 2003;234:203–210. [PubMed: 12824533]
30. Talos F, Petrenko O, Mena P, Moll UM. Mitochondrially targeted p53 has tumor suppressor activities in vivo. Cancer Res 2005;65(21):9971–9981. [PubMed: 16267022]
31. Moll UM, Wolff S, Speidel D, Deppert W. Transcription-independent pro-apoptotic functions of p53. Curr Opin Cell Biol 2005;17(6):631–636. [PubMed: 16226451]
32. Melino G, Bernassola F, Ranalli M, Yee K, Zong WX, Corazzari M, et al. p73 Induces apoptosis via PUMA transactivation and Bax mitochondrial translocation. J Biol Chem 2004;279(9):8076–8083. [PubMed: 14634023]
33. Shintani T, Klionsky DJ. Autophagy in health and disease: a double-edged sword. Science 2004;306 (5698):990–995. [PubMed: 15528435]
34. Jin S. p53, Autophagy and tumor suppression. Autophagy 2005;1(3):171–173. [PubMed: 16874039]
35. Degenhardt K, Mathew R, Beaudoin B, Bray K, Anderson D, Chen G, et al. Autophagy promotes tumor cell survival and restricts necrosis, inflammation, and tumorigenesis. Cancer Cell 2006;10(1): 51–64. [PubMed: 16843265]
36. Feng Z, Zhang H, Levine AJ, Jin S. The coordinate regulation of the p53 and mTOR pathways in cells. Proc Natl Acad Sci U S A 2005;102(23):8204–8209. [PubMed: 15928081]
37. Tasdemir E, Maiuri MC, Galluzzi L, Vitale I, Djavaheri-Mergny M, D'Amelio M, et al. Regulation of autophagy by cytoplasmic p53. Nat Cell Biol 2008;10(6):676–687. [PubMed: 18454141]
38. Di Leonardo A, Linke SP, Clarkin K, Wahl GM. DNA damage triggers a prolonged p53-dependent G1 arrest and long-term induction of Cip1 in normal human fibroblasts. Genes Dev 1994;8(21):2540–2551. [PubMed: 7958916]

Figure 1A: PUMA 4 hour

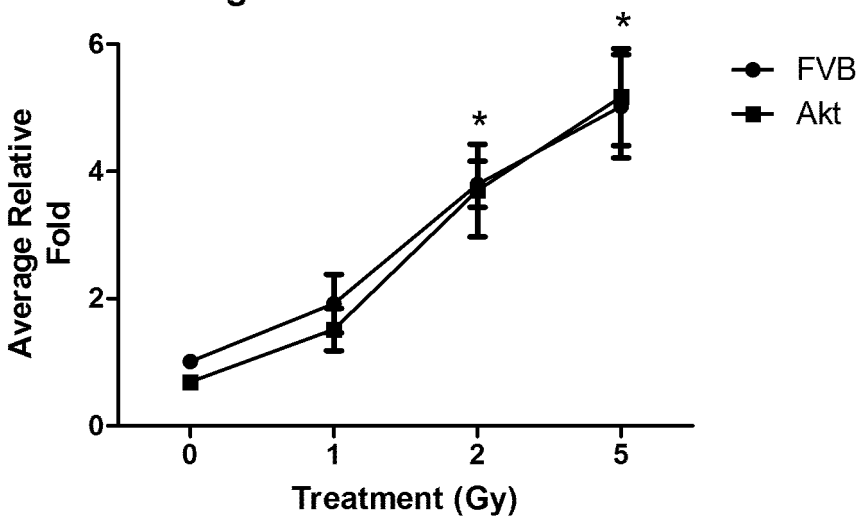

Figure 1B: PUMA 8 hour

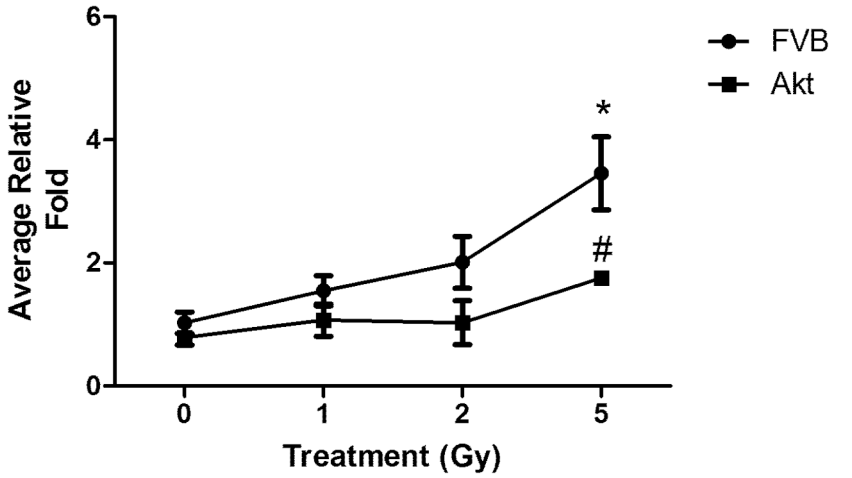

Figure 1C: Bax 4 hour

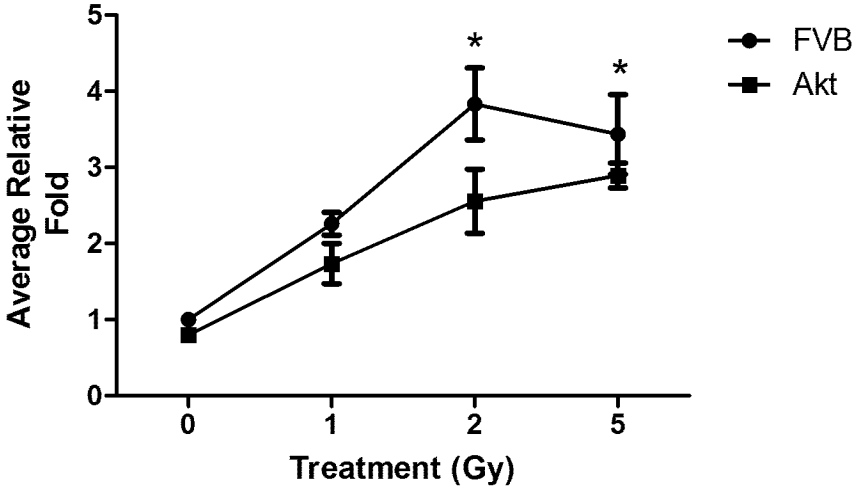

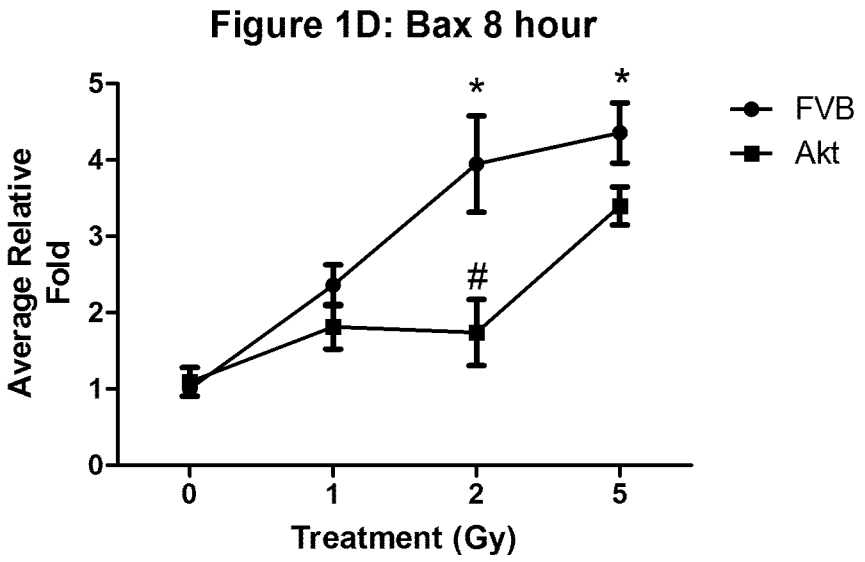

Figure 1. Induction of p53-dependent apoptotic genes in FVB wildtype and myr-Akt1 transgenic mice following radiation *in vivo*

The head and neck region of FVB wildtype and myr-Akt1 transgenic mice was exposed to 0, 1, 2, or 5 Gy radiation and the parotid salivary glands were removed 4 or 8 hours post-irradiation. PUMA or Bax expression was graphed using the $2^{-\Delta\Delta}$ C_t method and normalized to untreated wildtype. Induction of PUMA in FVB wildtype and myr-Akt transgenic mice at 4 (A) or 8 (B) hours. Induction of Bax in FVB wildtype and myr-Akt transgenic mice at 4 (C) or 8 (D) hours. Significant differences ($p \leq 0.05$) were determined using an ANOVA followed by a Bonferroni test adjusted for the number of pairwise comparisons. (*) indicates significant difference from the corresponding untreated genotype and (#) indicates significance between genotypes of the same treatment.

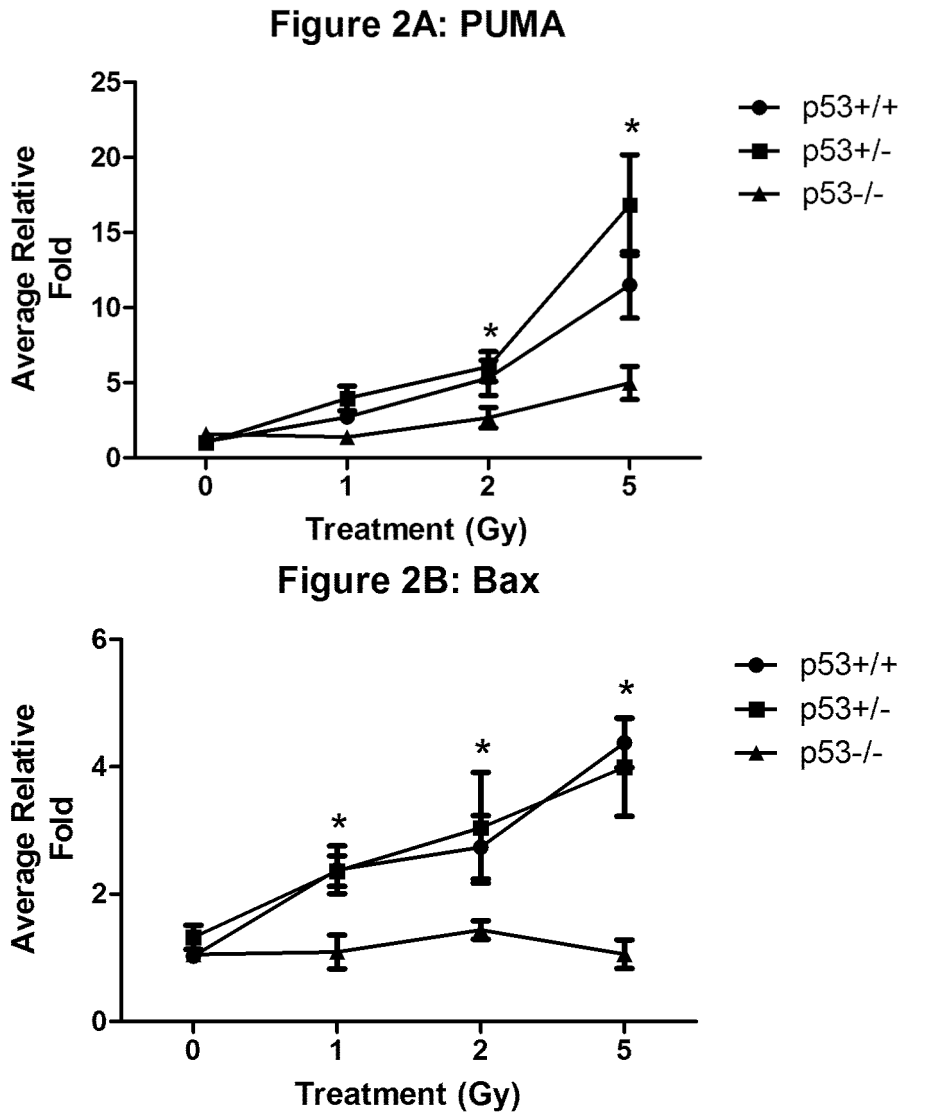

Figure 2. Induction of p53-dependent apoptotic genes in p53 mice following irradiation *in vivo*

The head and neck region of p53+/+, p53+/−, and p53−/− mice was exposed to 1, 2, or 5 Gy radiation and the parotid salivary glands were removed 4 hours post-irradiation. PUMA and Bax expression was analyzed as described in Figure 1. Induction of PUMA (A) and Bax (B) in p53 genotype mice. Significant differences ($p \leq 0.05$) were determined using an ANOVA followed by a pairwise Bonferroni test adjusting for the number of comparisons. (*) indicates significant difference from the corresponding untreated genotype.

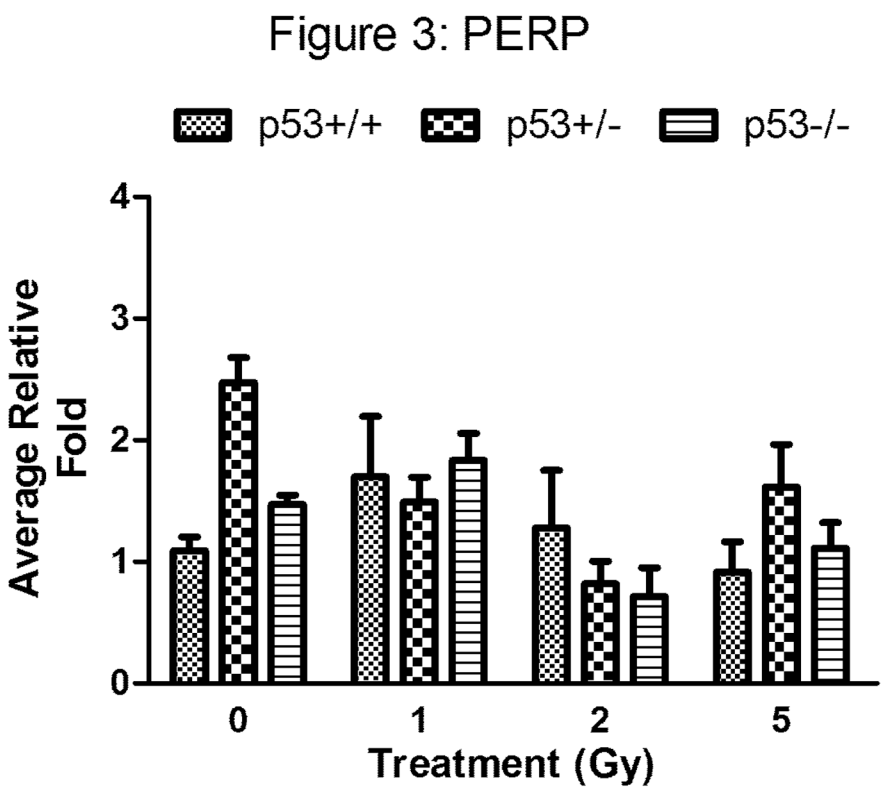

Figure 3. Analysis of PERP following irradiation *in vivo*

The head and neck region of p53+/+, p53+/−, and p53−/− mice was exposed to 1, 2, or 5 Gy radiation and the parotid salivary glands were removed 4 hours post-irradiation. PERP expression was analyzed as described in Figure 1.

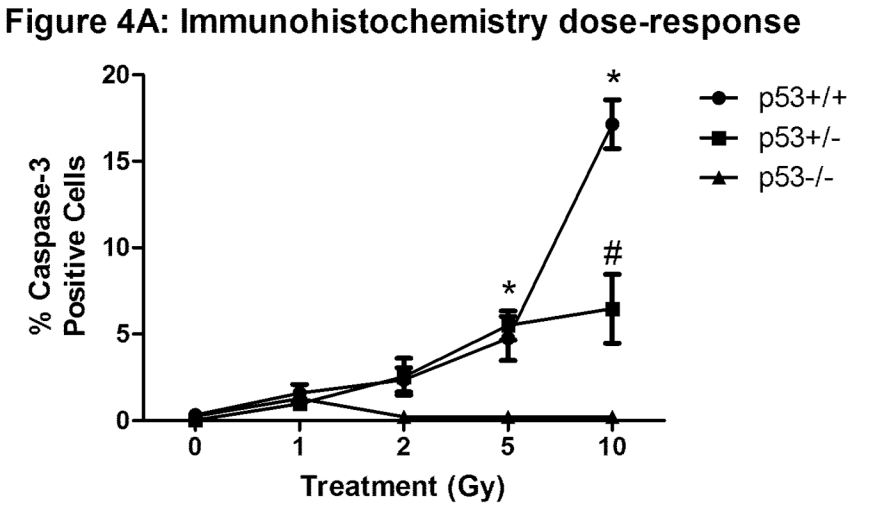

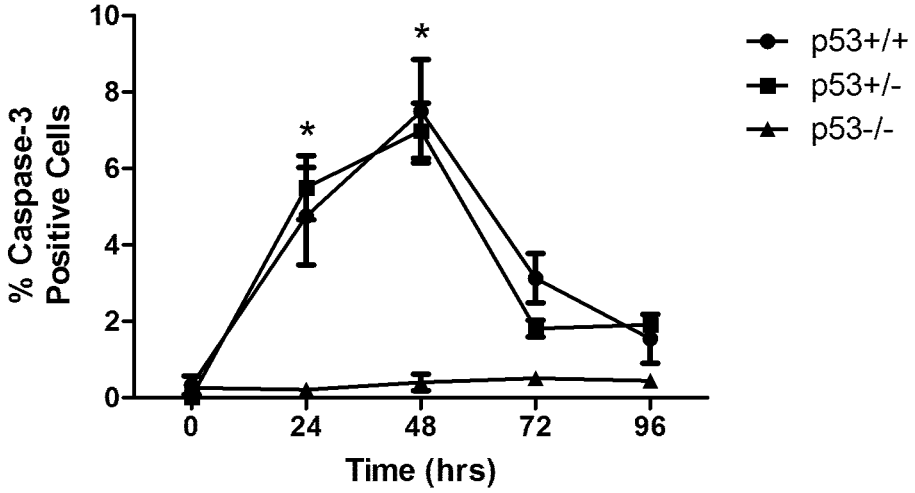

Figure 4. Reduced apoptosis in p53−/− mice following head and neck irradiation

In (A), the head and neck region of p53+/+, p53+/−, and p53−/− mice was exposed to 1, 2, 5, or 10 Gy radiation and the parotid salivary glands were removed 24 hours post-irradiation. The number of caspase-3 positive cells is graphed as a percentage of the total number of cells per field of view. In (B), four-week old female p53+/+, p53+/−, and p53−/− mice were exposed to 5 Gy radiation as described in (A) and parotid salivary glands were removed at 24, 48, 72, and 96 hours. Tissues were processed for activated caspase-3 immunohistochemistry as described in (A). The graph represents all data from three mice per group (exception: p53−/− mice were 2 mice per group). Significant differences ($p \leq 0.05$) were determined using an ANOVA followed by a pairwise Bonferroni test adjusting for the number of comparisons. (*) indicates significant difference from the corresponding untreated genotype and (#) indicates significance between genotypes of the same treatment.

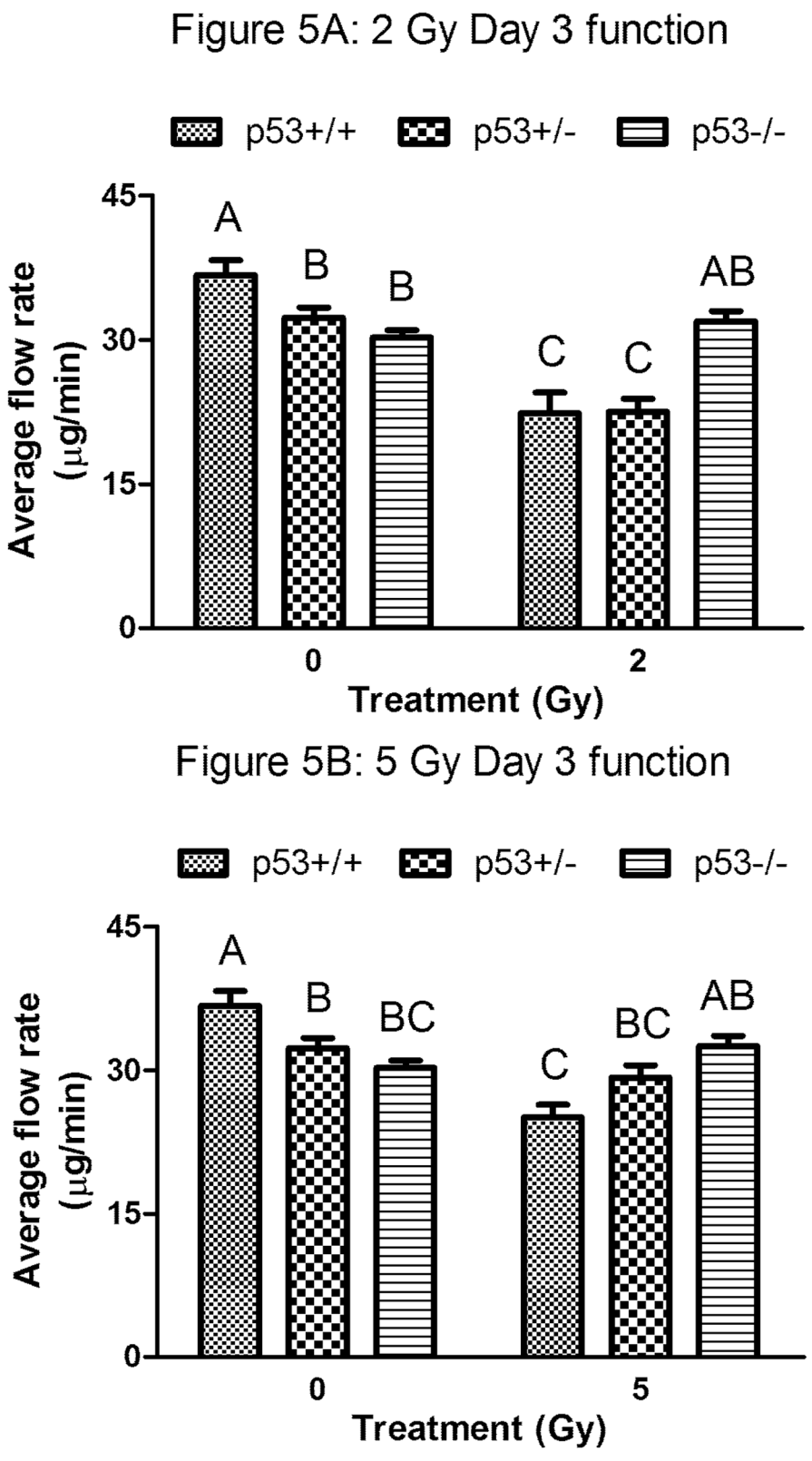

Figure 5. Acute salivary gland dysfunction 3 days after radiation exposure

p53+/+, p53+/−, and p53−/− mice were exposed to A) 2 Gy and B) 5 Gy radiation. Three days after exposure to radiation total saliva was collected following carbachol injection and graphed as μg/min. Graph A represents all data from at least eight mice/group and graph B represents all data from at least six mice/group. Significant differences ($p \leq 0.05$) were determined using an ANOVA followed by Tukey's multiple comparison LSD. Treatment groups with the same letters are not significantly different from each other.

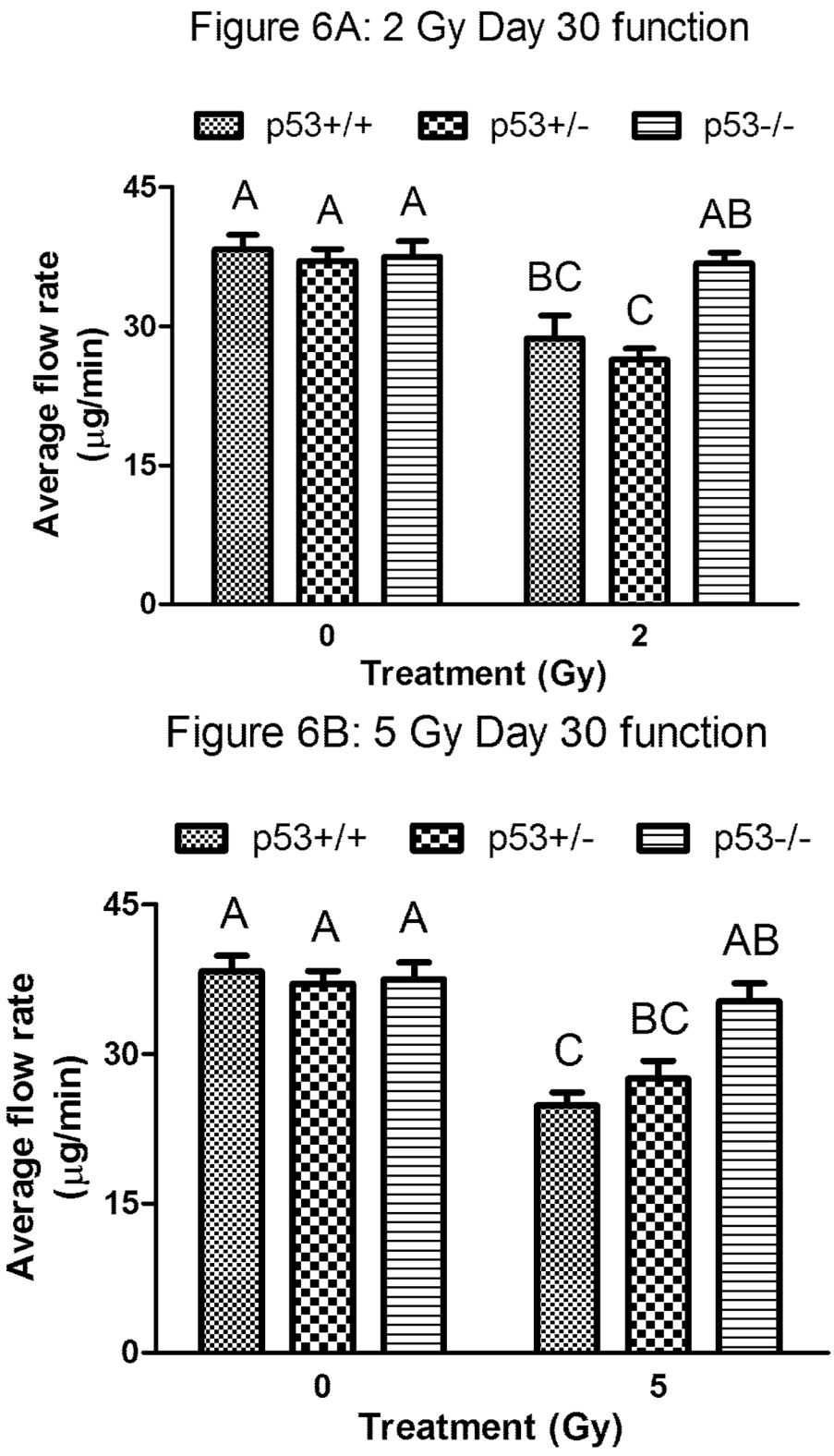

Figure 6. Chronic salivary gland dysfunction 30 days after radiation exposure

p53+/+, p53+/−, and p53−/− mice were exposed to A) 2 Gy and B) 5 Gy radiation. Thirty days after exposure to radiation total saliva was collected following carbachol injection and graphed as μg/min. Graph A represents all data from at least eight mice/group and graph B represents all data from at least six mice/group. Significant differences ($p \leq 0.05$) were determined using a One-Way ANOVA followed by Tukey's multiple comparison LSD. Treatment groups with the same letters are not significantly different from each other.